Targeting mitochondrial translation in RB1-deficient triple-negative breast cancer

Robert A. Jones[1, §], Tyler J. Robinson[1, §], Jeff C. Liu[1, §], Mariusz Shrestha[1,2, §], Veronique Voisin[3,§], YoungJun Ju[1], Philip E.D. Chung[1,2], Giovanna Pellecchia[2], Victoria L. Fell[1], SooIn Bae[4], Lakshmi Muthuswamy[5], Alessandro Datti[6.7], Sean E. Egan[8,9], Zhe Jiang[1], Gustavo Leone[4], Gary D. Bader[3,9], Aaron Schimmer[10] and Eldad Zacksenhaus[1,2,11*]

SUPPLEMENTARY TABLES S1-S2 and FIGURES S1-S14

Supplemental Table S1. Chromatin-immunoprecipitation (ChIP) data on E2F1 recruitment to MPT and cell cycle promoters in MCF10A and MCF7 cells

		ChIP-Seq (MCF7)		ChIP-Chip (MCF7, MCF10A)				
Gene	**Chrom**	**Peaks**	**Encode**	**Peaks Range**	**Ave ePV**	**MCF7**	**MCF10A**	***500bp**
SFXN1	chr5	169	169.149	(-165) -- (30)	0.02734	+	-	**Yes**
SFXN2	chr10	-43	165.207	(-257) -- (445)	0.01818	+	+	**Yes**
SMAD3	chr15	307	128.485	(-1258) – (-1113)	0.03377	+	-	No
MRPL37	chr1	-99	126.794	(-475) -- (340)	0.00976	+	+	**Yes**
TTC19	chr17	143	100.876	(18)	0.00800	-	+	**Yes**
HTRA2	chr2	200	99.748	(-382) -- (491)	0.02122	+	+	**Yes**
PARK7	chr1	-12	79.489	(-239) -- (-144)	0.02434	+	+	**Yes**
NSUN4	chr1	-342	77.904	(551)	0.00050	+	+	No
MRPL40	chr22	-151	76.814	(233) -- (478)	0.02894	+	+	**Yes**
CISD1	chr10	-460	57.495	(-523) -- (-143)	0.01591	+	+	**Yes**
ETFDH	chr4	-379	54.638	(-233) -- (-193)	0.01237	+	+	**Yes**
MPV17	chr2	79	51.905	(-248) -- (-173)	0.02611	+	+	**Yes**
PHB2	chr12	95	39.419	(-385) -- (116)	0.02034	+	+	**Yes**
DUSP18	chr22	-155	38.338	(-241) -- (-36)	0.00849	+	-	**Yes**
HIGD2A	chr5	70	36.271	(-399) -- (224)	0.00360	+	+	**Yes**
NDUFAB1	chr16	295	29.171	(-13) -- (127)	0.02427	+	+	**Yes**
TOMM40	chr19	-216	27.798	(-645) -- (-525)	0.00360	+	+	**Yes**
ATP5D	chr19	-27	25.273	(-220) -- (-100)	0.01764	+	+	**Yes**
MRPL43	chr10	165	15.703	(-206) -- (224)	0.01452	+	+	**Yes**
DHFR	chr5	350	4.057	(-605) -- (-415)	0.02249	+	+	No
TK1	chr17	39	12.113	(-688) -- (-188)	0.00985	+	+	**Yes**
POLA1	chrX	-93	29.955	(-610) -- (-325)	0.00718	+	+	**Yes**
CCNE1	chr19	128	73.359	(-954)	0.01000	+	-	No
CDK1	chr10	-695	12.265	(-551) -- (-136)	0.01133	+	+	**Yes**
ALB	chr4	NA	NA	NA	NA	NA	NA	NA

*** Peaks detected by ChIP-Seq and ChIP-Chip are within 500 bp of each other**

Supplemental Table S2. Correlation analysis of RB, E2F1 and E2F3 expression with those of indicated MPT vs known E2F-regulated cell cycle genes. Albumin was used as negative ctrl.

	RB	E2F1	E2F3
atp5d	**-0.11*** **	**0.06** **	0.01
cisd1	0	**0.10*** **	**0.08*** **
mprl37	**-0.22*** **	**0.28*** **	**0.21*** **
ndufab1	**-0.04***	**0.06** **	-0.11
nsun4	**-0.18*** **	**0.17*** **	**0.14*** **
phb2	**-0.20*** **	**0.04***	**0.16*** **
sfxn1	-0.01	**0.05***	-0.02
smad3	-0.03	**0.18*** **	**0.05***
tomm40	**-0.26*** **	**0.20*** **	**0.37*** **
dhfr	-0.04	**0.08*** **	**0.13*** **
tk1	**-0.17*** **	**0.22*** **	**0.21*** **
Pola1	**-0.13*** **	**0.12*** **	**0.09*** **
Ccne1	**-0.17*** **	**0.20*** **	**0.35*** **
cdc2	-0.02	**0.13*** **	**0.17*** **
alb	0.03	0.01	**-0.10*** **

+ve / **-ve** Correlation

*p < 0.05; **p <0.005; ***p < 0.0005

MFS	#Basal Patient	Treatment
GSE2034	52	Radiotherapy
GSE2603	22	Radiotherapy
GSE5327	35	<unknown>
GSE6532	18	Tamoxifen
GSE11121	25	Radiotherapy
GSE25066	189	taxane-anthracycline chemotherapy

Supplemental Figure S1

Figure S1. Cohorts with Metastasis Free Survival (MFS) and RNA expression data used for bioinformatic analysis. These breast cancer datasets were combined for the bioinformatic analysis shown in Fig 1. Treatment and number of basal-like patients in each cohort (based on PAM50 classification) are indicated.

A

Tumor Model	Mammary Tumor Incidence	Median Tumor Onset
MMTV*cre*:Rb$^{f/f}$:p53$^{f/f}$ (Transplant)	6/8 donors (75%) 19/26 transplants (73%)	275
MMTV*cre*:Rb$^{f/f}$:p53$^{f/f}$	16/21 (76%)	453
Ad-CMV*cre*:Rb$^{f/f}$:p53$^{f/f}$	3/3 experiments (100%) 6/9 transplants (67%)	261
MMTV*cre*:Rb$^{f/f}$:p53$^{LSLR270H/+}$	5/10 (50%)	429

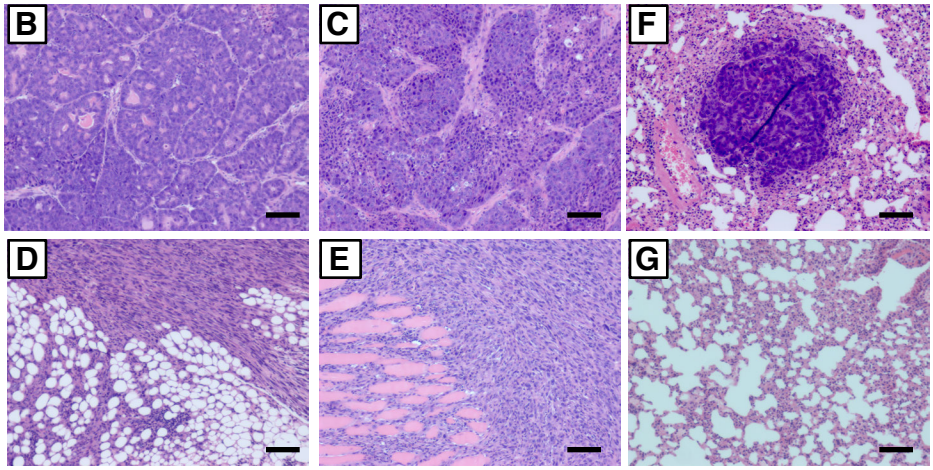

WAP*cre*;Rb$^{f/f}$;p53$^{f/f}$

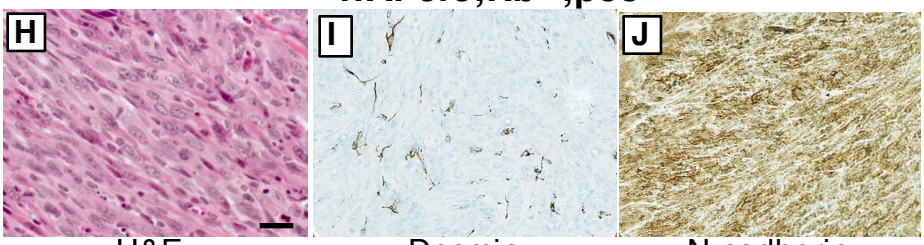

H&E Desmin N-cadherin

Supplemental Figure S2

Figure S2. Disruption of Rb and p53 in mammary epithelium via MMTV-cre or WAP-Cre induces spindle-cell tumors. **(A)** Incidence and onset of mammary tumor formation in indicated models following disruption of Rb and p53 in mammary epithelia. (**B-C**, **F**) Histology of rare solid mammary tumors that developed in two MMTV*cre*;$Rb^{f/f}$;$p53^{f/f}$ mice and a corresponding lung metastases (F) from (B). **(D-E, G)** Locally invasive spindle cell tumors without lung metastases (G) from MMTV*cre*;$Rb^{f/f}$;$p53^{f/f}$ mice. **(H-J)** Histology and expression of the mesenchymal markers desmin and N-cadherin in a spindle-cell tumor from WAP*cre*;$Rb^{f/f}$;$p53^{f/f}$ mice. Scale bars in B-G, 200μm; H, 50μm.

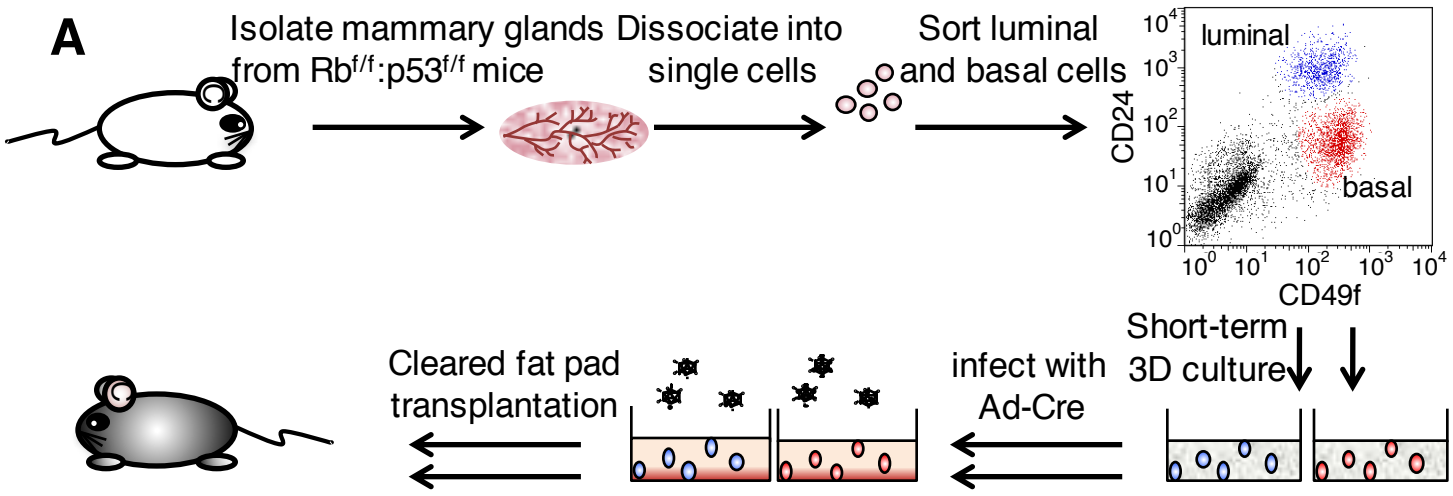

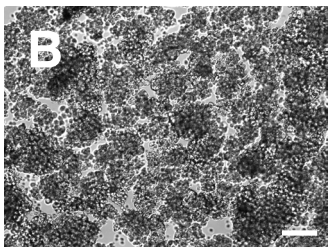

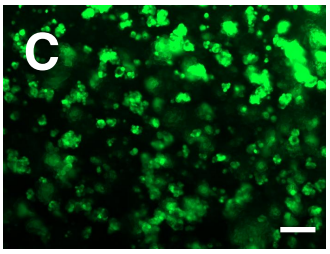

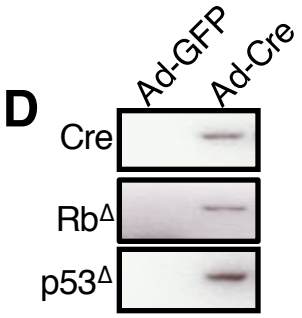

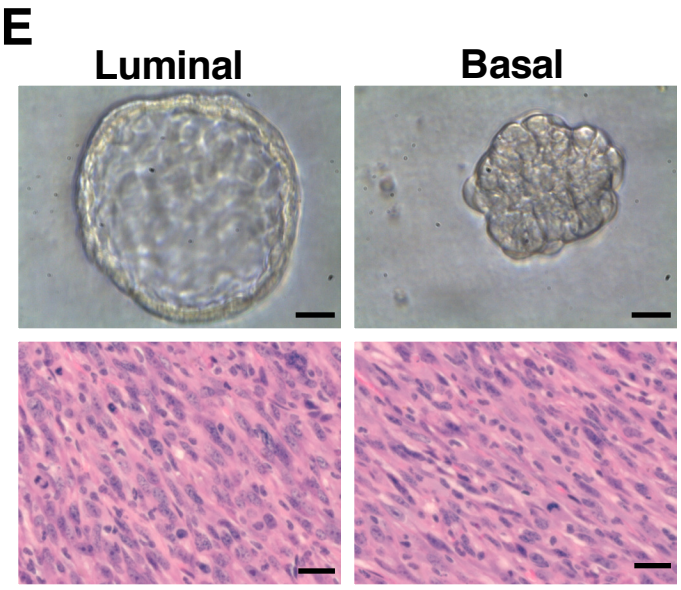

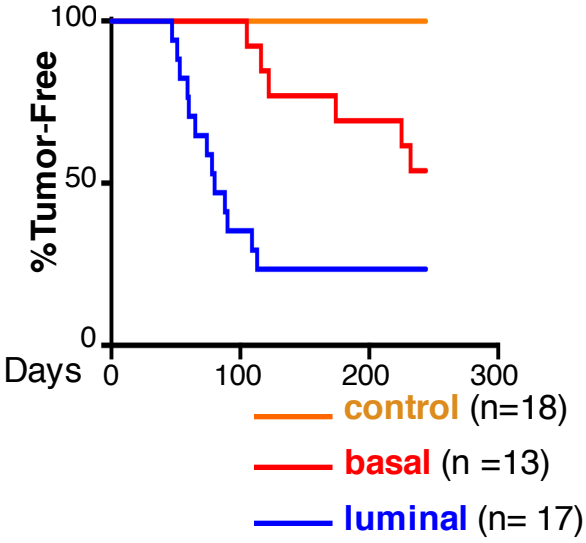

G

Experiment		#Tumors/#Mice Luminal	Basal	Control
with support cells	1	5/5	3/5	0/3
	2	2/3	1/3	0/3
	3	3/3	1/3	0/3
without support cells	4	1/2	1/2	N/A
	5	2/4	N/A	N/A
	total	13/17 (76%)	6/13 (46%)	0/9

Supplemental Figure S3

Figure S3. Disruption of Rb and p53 in enriched populations of either luminal or basal progenitors induce spindle-tumors. (**A**) Schematic of the experimental protocol used to delete Rb and p53 in luminal or basal progenitors. Primary mammary epithelial cells (MECs) were isolated from $Rb^{f/f}$;$p53^{f/f}$ mice and sorted into luminal and basal cell populations using fluorescent activated cell sorting (FACS). Sorted cells were then cultured in 3D to allow formation of sphere-like organoids. After 5-8 days, organoids were dissociated into single cells, infected with Ad-*cre*-GFP and transplanted into cleared fat pads of immune-deficient mice. (**B-D**) *Ex vivo* deletion of Rb and p53. Brightfield (B) and GFP fluorescent (C) photomicrographs of Ad-*cre*-GFP infected primary $Rb^{f/f}$;$p53^{f/f}$ mammary epithelial cells cultured under non-adherent conditions. Scale bars 100μm. (D) PCR analysis for Rb and p53 recombination 72hrs post infection with Ad-*cre*-GFP or Ad-GFP. **(E) Top**, photomicrographs showing distinct morphologies of luminal and basal organoids in 3D conditions (scale bars, 20μm). **Bottom**, histology of mammary tumors developed following Ad-*cre*-GFP mediated deletion of $Rb^{f/f}$ and $p53^{f/f}$ in luminal or basal progenitors. **(F)** Kaplan-Meier mammary tumor-free survival curves of mice transplanted with Rb/p53-deficient luminal or basal progenitors (Fisher's exact test, p=0.1322). Ad-GFP infected cells from wild type mice served as controls. **(G)** Tumor incidence from the Ad-*cre*-GFP -infected $Rb^{f/f}$;$p53^{f/f}$ luminal or basal progenitors.

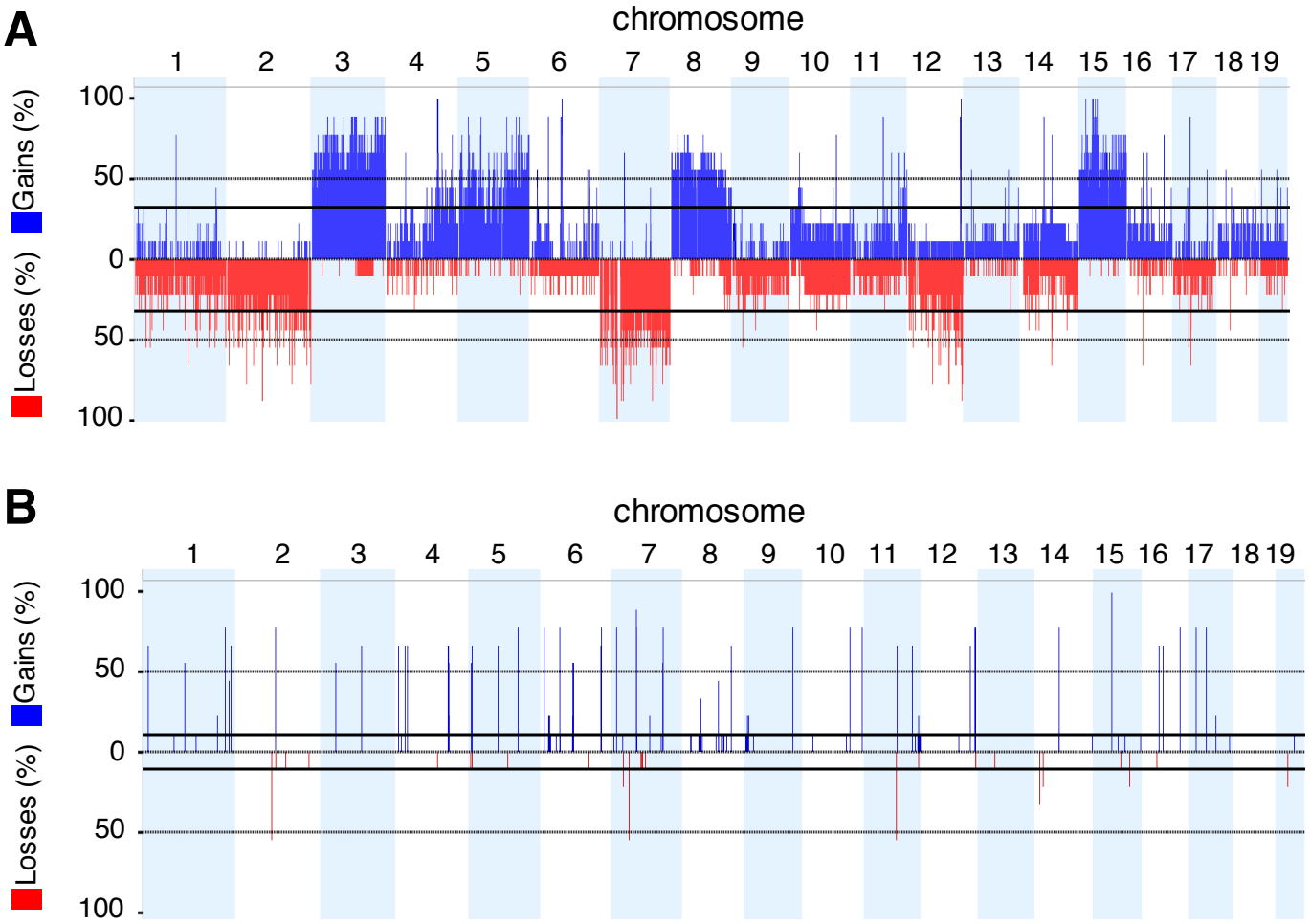

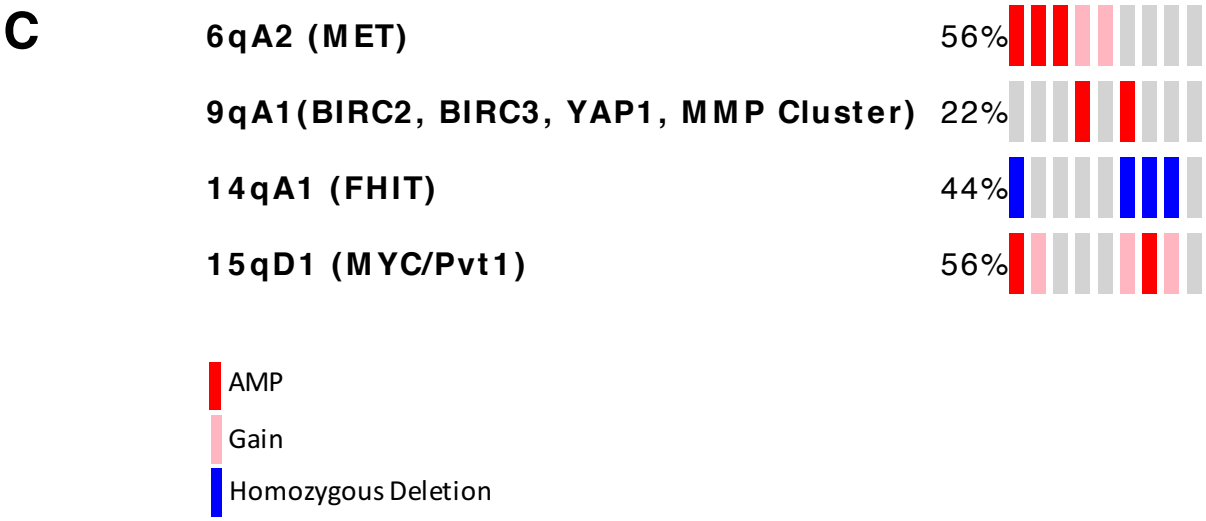

Supplemental Figure S4A-C

D

Region	Region Length	Cytoband Location	Event
chr1:90,194,440-90,208,356	13916	qD	CN Gain
chr2:77,709,806-77,867,695	157889	qC3	CN Loss
chr4:111,738,147-112,270,058	531911	qD1	CN Gain
chr4:112,468,339-112,481,282	12943	qD1	CN Gain
chr4:112,509,281-113,255,950	746669	qD1	CN Gain
chr4:113,544,283-113,585,504	41221	qD1	CN Gain
chr6:17,054,902-17,711,820	656918	qA2	CN Gain
chr6:17,849,280-18,003,078	153798	qA2	CN Gain
chr6:19,938,904-21,000,795	1061891	qA2	CN Gain
chr6:41,017,660-41,115,088	97428	qB1	CN Gain
chr6:70,448,376-70,628,523	180147	qC1	CN Gain
chr7:26,778,136-26,984,188	206052	qA3	CN Loss
chr7:38,963,263-38,985,946	22683	qB2	CN Loss
chr7:54,893,308-54,997,383	104075	qB4	CN Gain
chr9:6,557,813-8,368,369	1810556	qA1	CN Gain
chr9:9,153,878-9,190,123	36245	qA1	CN Gain
chr10:100,595,649-100,669,755	74106	qD1	CN Gain
chr11:70,982,720-71,111,487	128767	qB4	CN Gain
chr11:103,370,441-103,390,309	19868	qE1	CN Gain
chr11:116,602,137-116,629,157	27020	qE2	CN Gain
chr12:114,835,050-114,971,111	136061	qF1	CN Gain
chr12:115,303,388-115,378,652	75264	qF1	CN Gain
chr12:115,864,896-116,024,653	159757	qF2	CN Gain
chr12:116,264,299-116,299,818	35519	qF2	CN Gain
chr14:10,729,542-11,668,820	6063	qA1	CN Loss
chr14:52,575,120-52,593,014	17894	qC2	CN Gain
chr15:61,050,340-62,788,961	1738621	qD1	CN Gain
chr16:36,244,633-36,328,140	83507	qB3	CN Gain
chr16:44,830,484-44,868,563	38079	qB4	CN Gain
chr16:80,943,011-80,972,831	29820	qC3.3	CN Gain
chr17:38,441,884-38,514,425	72541	qB1	CN Gain

Supplemental Figure S4D

Figure S4. Copy number alterations in $Rb^{\Delta/\Delta}$;$p53^{\Delta/\Delta}$ claudin-low tumors. (**A-B**) Frequency plots of copy number alterations (amplification or homozygous deletion) in $Rb^{\Delta/\Delta}$;$p53^{\Delta/\Delta}$ mammary tumors at low (A) and high (B) stringency. (**C**) Oncoprint of copy number changes involving the indicated oncogenes and tumor suppressors. (**D**) Summary of high-level amplifications and homozygous deletions.

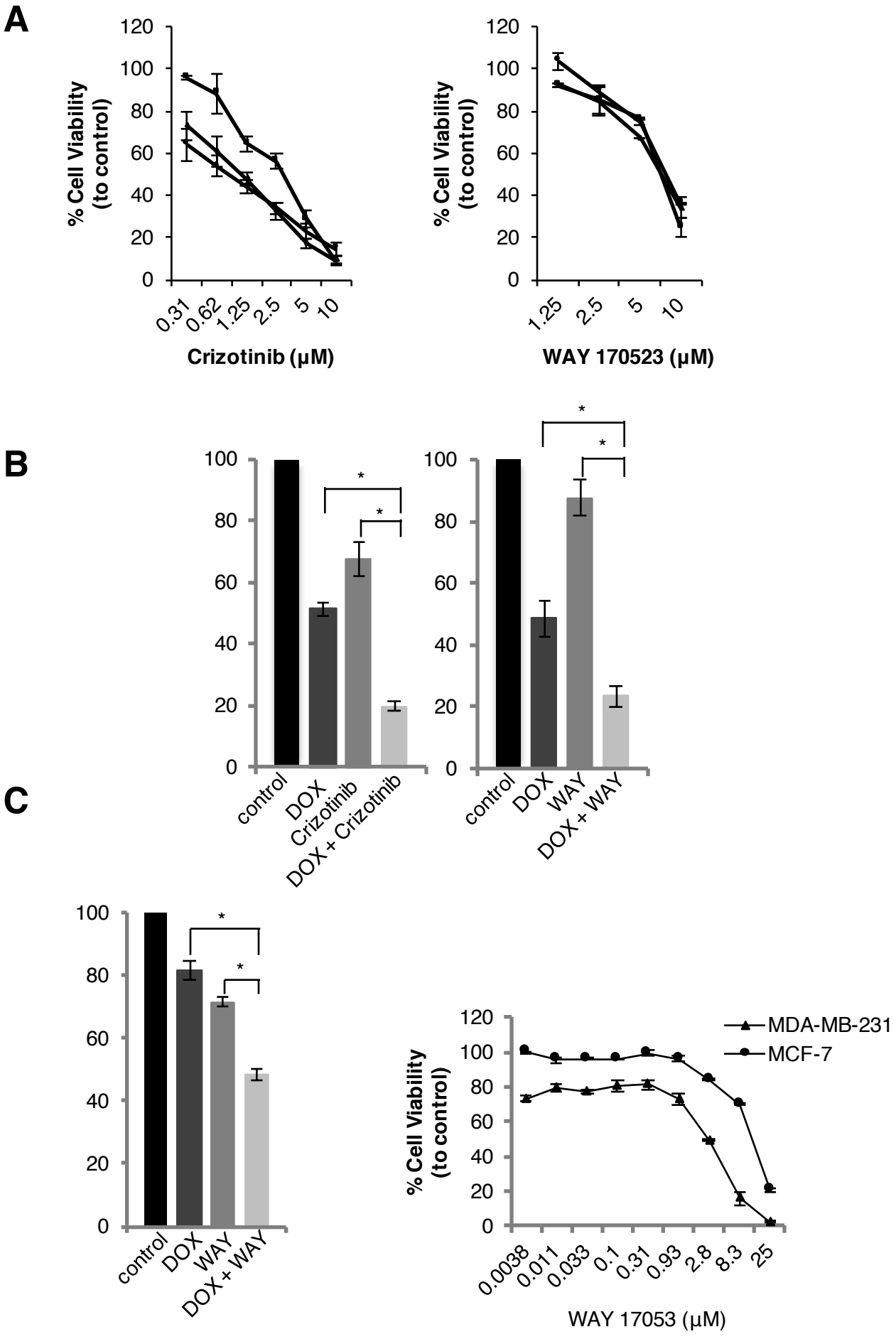

Supplemental Figure S5

Figure S5. **Effects of drugs that target amplified genes identified by aCGH analysis of $Rb^{\Delta/\Delta}$;$p53^{\Delta/\Delta}$claudin low-like tumors. (A)** Effect of the MET inhibitor crizotinib or the MMP13 inhibitor WAY170523 on $Rb^{\Delta/\Delta}$;$p53^{\Delta/\Delta}$ tumor cell viability (line# 1; MTT assay) 72 hr post treatment. (**B**) Effect of doxorubicin (DOX) alone or in combination with Crizotinib or WAY170523 on $Rb^{\Delta/\Delta}$;$p53^{\Delta/\Delta}$ tumor cell viability. (**C**) Effect of doxorubicin plus WAY170523 on viability of the claudin-low TNBC line, MDA-MB-231, and comparison to sensitivity of the luminal BC line, MCF7, showing increased sensitivity of TNBC cells.

A

Gene ID(s)	Ensembl ID(s)	Chr	Start	End	Strand	Nearest TSS	TFBS Start	TFBS End	TFBS Rel. Start	TFBS Rel. End	TFBS Strand	Abs. Score	Rel. Score	TFBS Sequence
Etfdh	ENSMUSG00000027809	3	79407710	79432785	-	79432785	79433023	79433030	-245	-238	+	8.832	87.00%	TTGGGCGC
Htra2	ENSMUSG00000068329	6	83001260	83005267	-	83005267	83006604	83006611	-1344	-1337	-	9.128	88.00%	TTTGTCGC
						83005267	83007079	83007086	-1819	-1812	-	8.832	87.00%	TTTGGGGC
Sfxn1	ENSMUSG00000021474	13	54167214	54203715	+	54167214	54167625	54167632	412	419	-	8.329	85.30%	TTGCGCGC
Higd2a	ENSMUSG00000025868	13	54691568	54692519	+	54691568	54691430	54691437	-138	-131	-	8.329	85.30%	TTGCGCGC
Rab3a	ENSMUSG00000031840	8	73278578	73282576	+	73278578	73277291	73277298	-1287	-1280	+	8.832	87.00%	ATTGGCGC
Smad3	ENSMUSG00000032402	9	63494574	63605801	-	63559776	63560901	63560908	-1132	-1125	-	8.832	87.00%	TTTGGGGC
						63605801	63605852	63605859	-58	-51	+	8.832	87.00%	TTTGGTGC
						63605801	63605988	63605995	-194	-187	+	8.624	86.30%	TTTCACGC
Mtx1	ENSMUSG00000064068	3	89013003	89031010	-	89014758	89014787	89014794	-36	-29	+	8.832	87.00%	TTTGGAGC
						89031010	89031210	89031217	-207	-200	-	8.832	87.00%	TCTGGCGC
						89031010	89031433	89031440	-430	-423	+	8.832	87.00%	TTTGGTGC
Ndufab1	ENSMUSG00000030869	7	129228917	129245400	-	129245220	129245146	129245153	68	75	-	8.496	85.90%	TTTGCCGG
Mrpl43	ENSMUSG00000025208	19	45079504	45080932	-	45080932	45081394	45081401	-469	-462	-	8.469	85.80%	TTTCGCGT
						45080932	45081709	45081716	-784	-777	+	8.832	87.00%	CTTGGCGC
						45080932	45082026	45082033	-1101	-1094	-	8.832	87.00%	TTTGGCCC
						45080932	45082586	45082593	-1661	-1654	-	8.329	85.30%	TTTCGAGC
Atp5d	ENSMUSG00000003072	10	79601377	79608563	+	79601377	79601715	79601722	339	346	-	8.329	85.30%	TGTCGCGC
Sfxn2	ENSMUSG00000025036	19	46647855	46671388	+	46647855	46647445	46647452	-410	-403	+	8.329	85.30%	TTACGCGC
						46647855	46647701	46647708	-154	-147	-	12.603	100.00%	TTTGGCGC
Nsun4	ENSMUSG00000028706	4	115704379	115726481	-	115726481	115725813	115725820	662	669	-	8.832	87.00%	TGTGGCGC
						115726481	115727690	115727697	-1216	-1209	-	8.832	87.00%	TTTGGCTC
Nsun4	ENSMUSG00000090697	4	115706512	115725985	-	115725985	115727690	115727697	-1712	-1705	-	8.832	87.00%	TTTGGCTC
Park7	ENSMUSG00000028964	4	150271242	150288546	-	150288315	150288400	150288407	-92	-85	-	8.329	85.30%	GTTCGCGC
Armcx3	ENSMUSG00000049047	X	131291134	131295994	+	131291186	131291630	131291637	445	452	-	10.444	92.60%	TTTCCCGC
Tomm40	ENSMUSG00000002984	7	20286662	20300787	-	20300787	20300802	20300809	-22	-15	+	10.444	92.60%	TTTCCCGC
						20300787	20301533	20301540	-753	-746	+	8.832	87.00%	TTTGGCCC
Phb2	ENSMUSG00000004264	6	124662340	124666968	+	124662340	124662161	124662168	-179	-172	-	8.329	85.30%	TTTCGAGC
Ttc19	ENSMUSG00000042298	11	62094975	62141953	+	62094975	62094760	62094767	-215	-208	+	8.329	85.30%	TCTCGCGC
Poldip2	ENSMUSG00000001100	11	78325695	78336238	+	78325695	78325569	78325576	-126	-119	-	8.329	85.30%	GTTCGCGC
Dusp18	ENSMUSG00000047205	11	3795243	3801299	+	3795243	3794364	3794371	-879	-872	-	8.832	87.00%	TTTGGTGC
Ppp1cc	ENSMUSG00000004455	5	122608287	122625282	+	122608287	122608059	122608066	-228	-221	-	8.832	87.00%	GTTGGCGC
						122608287	122608114	122608121	-173	-166	+	10.152	91.60%	TTTGGCGG
Mrpl40	ENSMUSG00000022706	16	18872111	18876860	-	18876860	18877050	18877057	-197	-190	-	8.329	85.30%	ATTCGCGC
						18876860	18877284	18877291	-431	-424	+	10.444	92.60%	TTTCCCGC
Mpv17	ENSMUSG00000090262	5	31443033	31460526	-	31460526	31459790	31459797	730	737	+	8.832	87.00%	TTTGGGGC
						31460526	31461820	31461827	-1301	-1294	+	9.648	89.80%	TTTCGCGG
Cisd1	ENSMUSG00000037710	10	70793228	70807702	-	70807702	70807718	70807725	-23	-16	+	8.832	87.00%	TTAGGCGC
Slc25a22	ENSMUSG00000019082	7	148615638	148623791	-	148623791	148624691	148624698	-907	-900	+	8.832	87.00%	TCTGGCGC
						148623791	148625646	148625653	-1862	-1855	-	8.832	87.00%	TTTGGCCC
Mrpl37	ENSMUSG00000028622	4	106728479	106739473	-	106737962	106738439	106738446	-484	-477	+	8.832	87.00%	TTTGGCTC

Supplemental Figure S6A

B

E2F mediated regulation of DNA replication

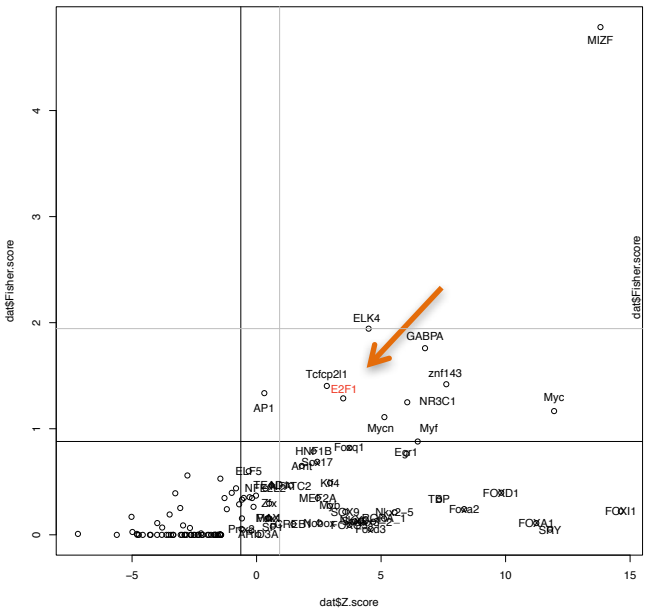

GST transferase

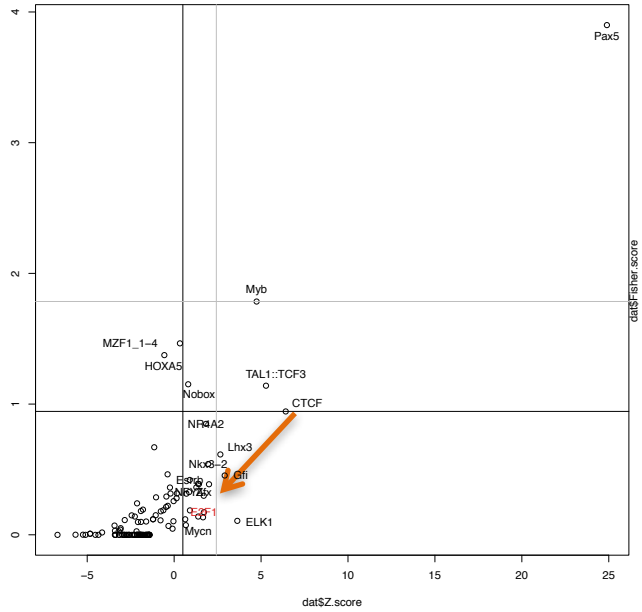

TCA

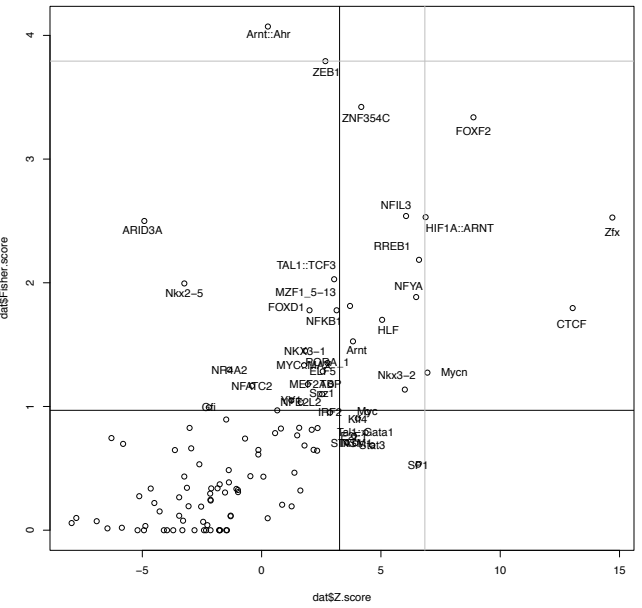

Supplemental Figure S6B

C

MRPL37

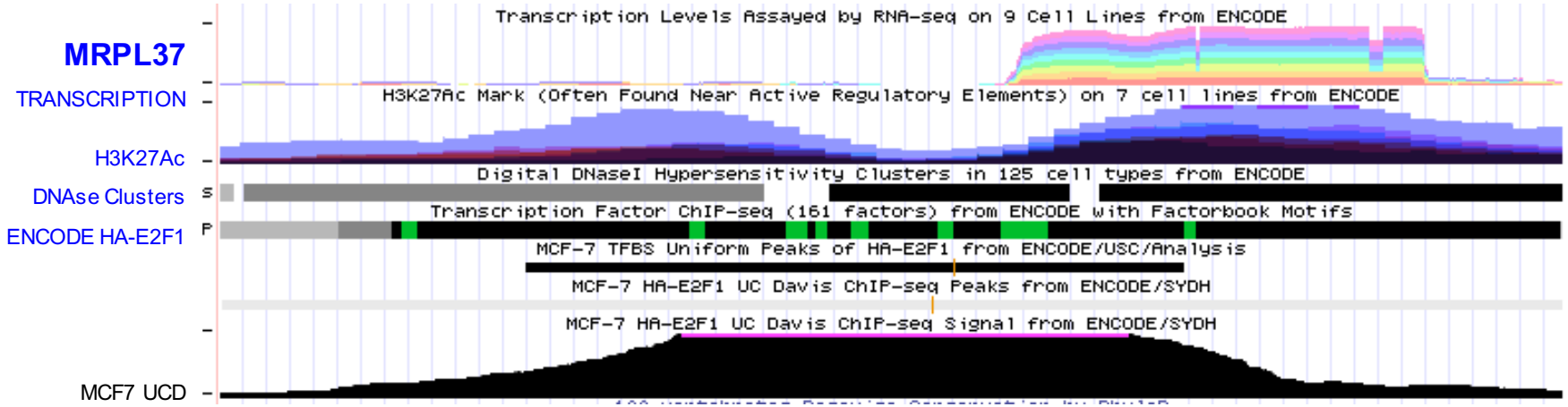

Supplemental Figure S6C

D

NSUN4

PHB2

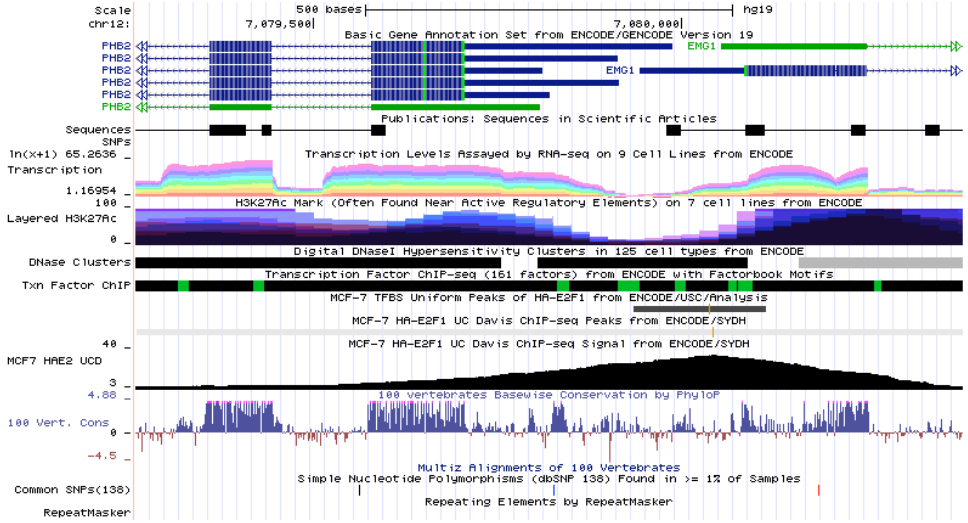

TOMM40

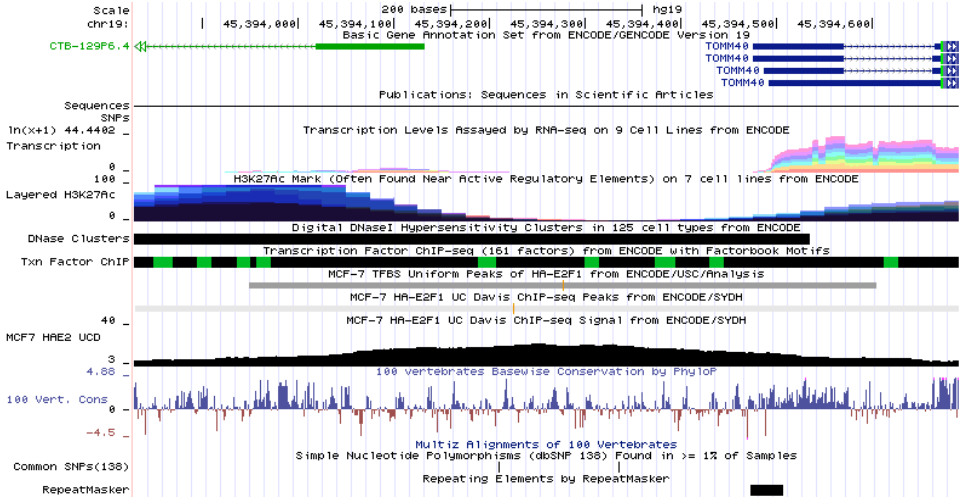

ATP5D

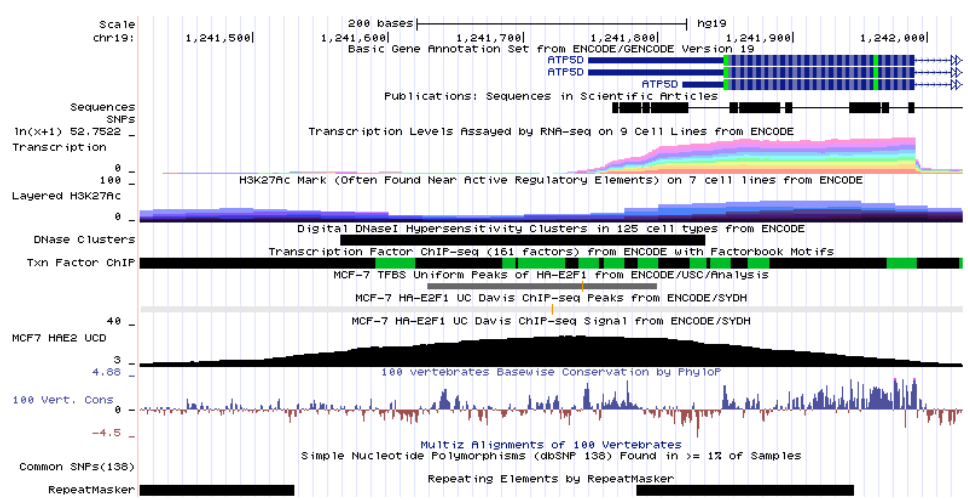

Supplemental Figure S6D

Figure S6. Control of mitochondrial protein translation genes by RB and E2F1. (**A**) A list of 26 MPT genes that are upregulated in Rb/p53-deficient vs. p53-deficient claudin-low like mammary tumors, and contain consensus E2F1 binding motif(s) in their promoters within -2kb to +1kb of the transcription starting site as deduced from oPOSSUM 3.0. Locations, scores and E2F sequences are indicated. (**B**) oPOSSUM analysis of E2F regulated DNA replication, GST transferase and TCA cycle genes. Note that E2F1 scored high only in the former pathway. (**C**) UCSC analysis of the MRPL37 gene depicting transcription, H3K27acetylation (Ac), DNA hypersensitive regions, E2F1 consensus binding sites and ChIP-seq data. (**D**) UCSC analysis of additional MPT genes (NSUN4, PHB2, TOMM40 and ATP5D) upregulated in Rb/p53 vs. p53 claudin-low like tumors and scored positive by ENCODE analysis of MCF7 cells. Note transcription from RNA-seq data, E2F1 consensus sites, DNase hypersensitive regions, ENCODE HA-E2F1 binding and H3K27acetylation mark suggesting active promoters.

A

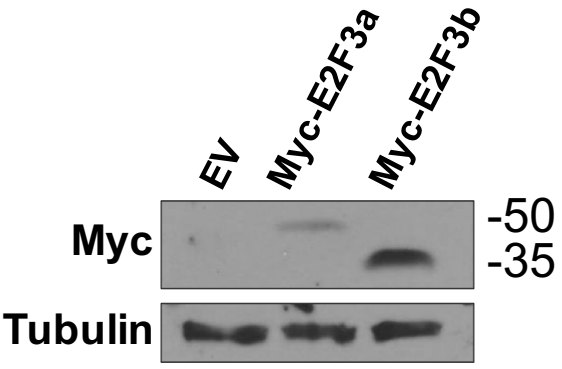

B

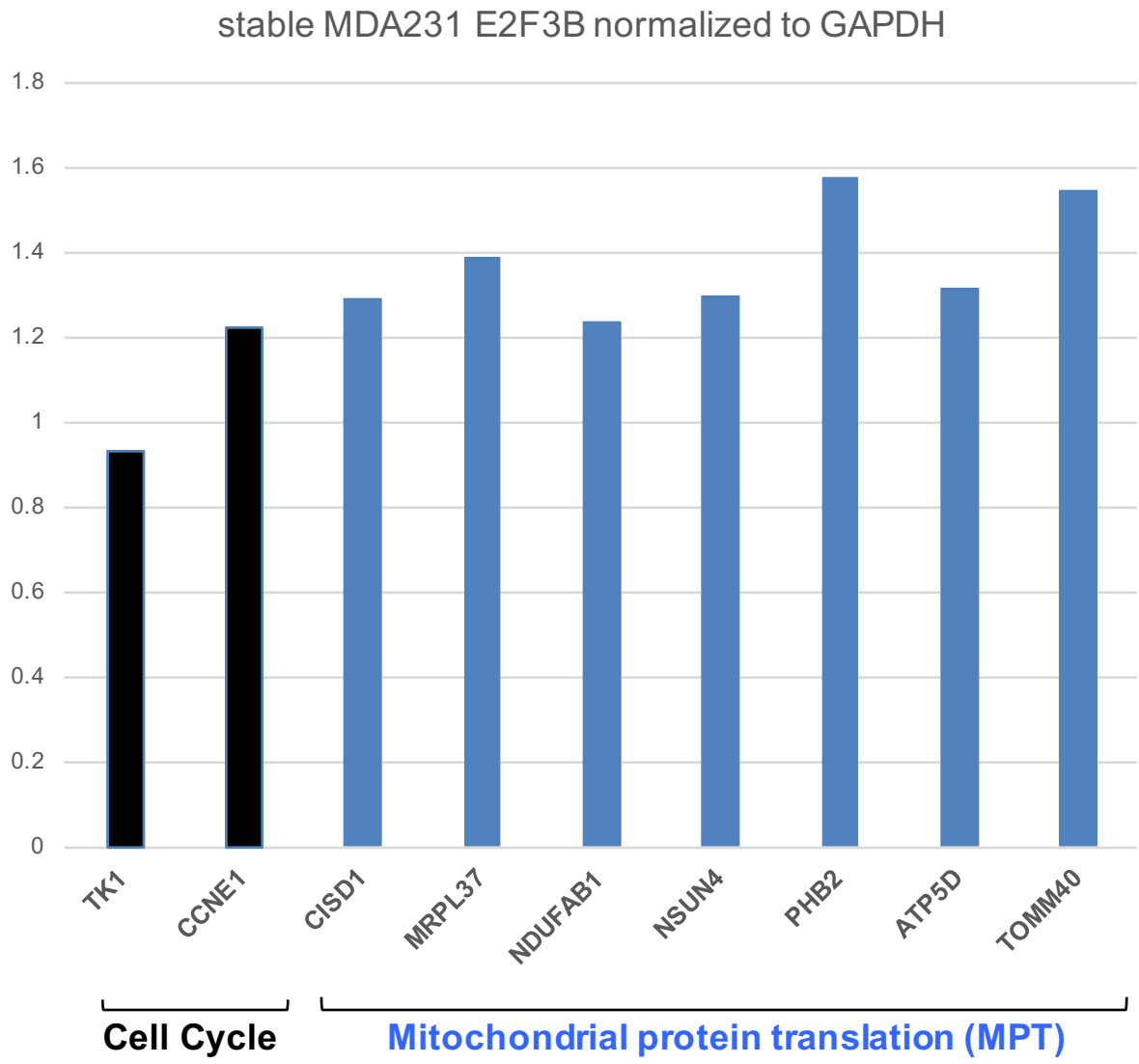

Supplemental Figure S7

Figure S7. **Moderate induction of MPT and cell cycle genes in MDA-MB-231 cells stably expressing E2F3b**. (**A**) Immunoblot of MDA-MB-231 cells stably transduced by retroviruses encoding Myc-E2F3a and Myc-E2F3b, or empty vector (EV). Note very low expression of Myc-E2F3a, and robust expression of the shorter, Myc-E2F3b protein. (**B**) Q-rt-PCR of indicated MPT and known E2F regulated cell cycle genes normalized for GAPDH in Myc-E2F3b-expressing MDA-MB-231 cells.

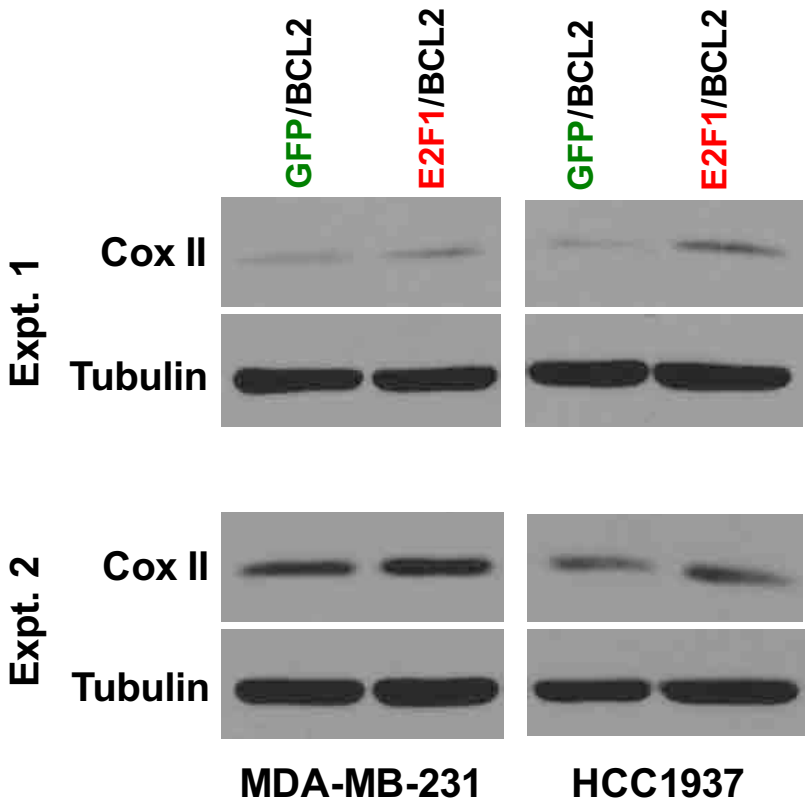

Supplemental Figure S8

Figure S8. **E2F1 induction of COX II protein expression in BC cells**. Two independent experiments showing the induction of the mitochondrially translated protein COX II in the indicated TNBC lines transduced by adenovirus vectors encoding E2F1 or GFP alone (control) together with Ad.Bcl-2.

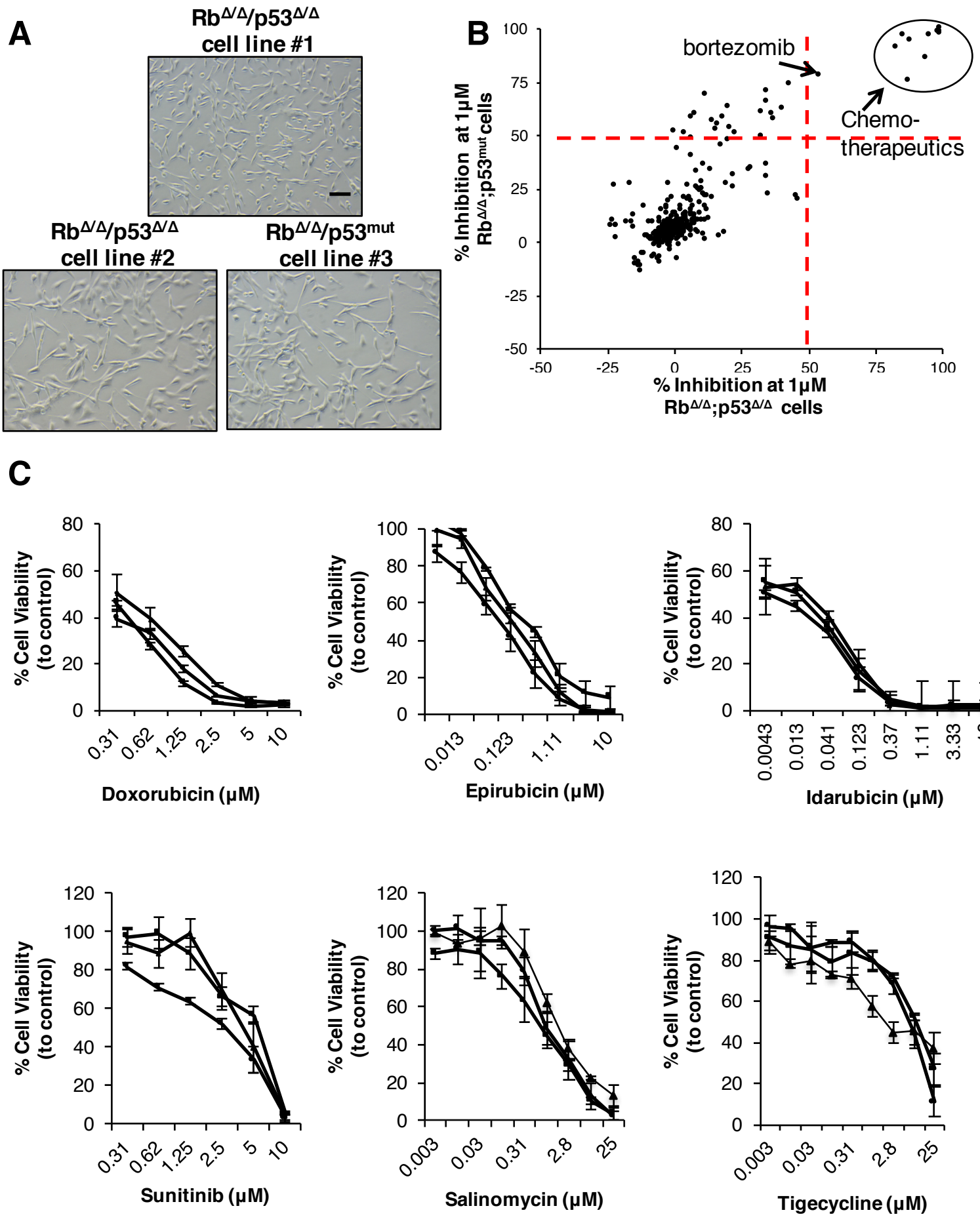

Supplemental Figure S9A-C

Figure S9. **High-throughput screen of FDA-approved drugs identifies potential therapeutic for claudin-low TNBC**. (**A**) Photomicrographs of primary mammary tumor cell lines isolated from Rb/p53-deficient ($Rb^{\Delta/\Delta}$;$p53^{\Delta/\Delta}$; cell lines #1-2) or Rb deficient/p53 mutant ($Rb^{\Delta/\Delta}$;$p53^{mut/+}$; cell line #3) tumors. Scale bars, 200μm. (**B**) Scatter plot of high-throughput screening data showing % inhibition of cell viability following treatment with compounds from the FDA-approved library at 1μM. (**C**) Validation of drugs identified in the 10μM FDA-approved drug screen (Fig. 8C). Effects of doxorubicin, epirubicin, idarubicin, sunitinib, salinomycin and tigecycline on Rb/p53-deficient (#1 (●) and #2 (■)) and Rb-deficient/p53 mutant (#3, ▲) primary mammary tumor cells lines.

A

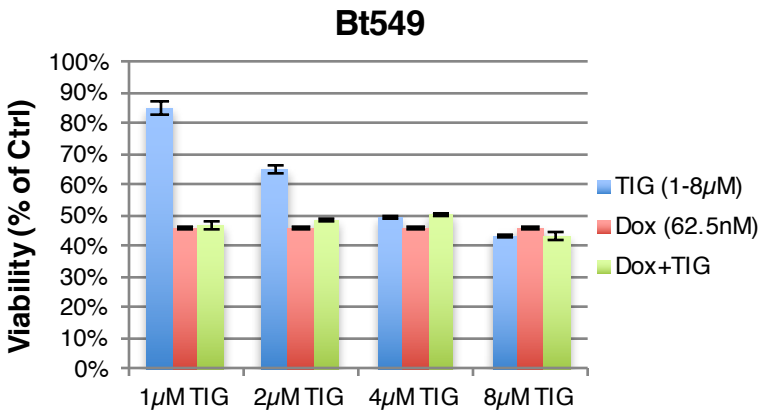

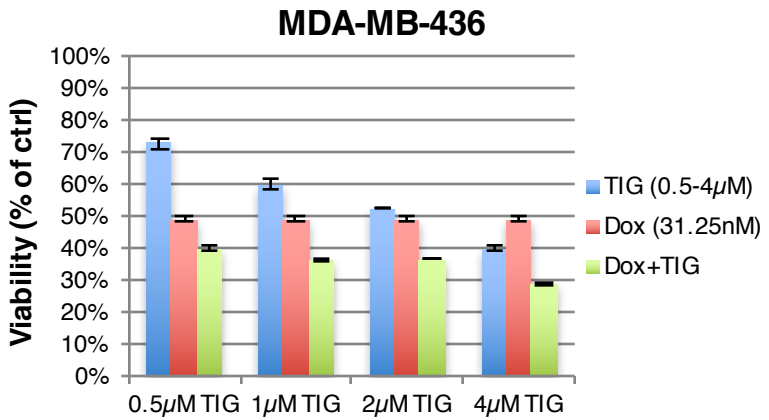

B

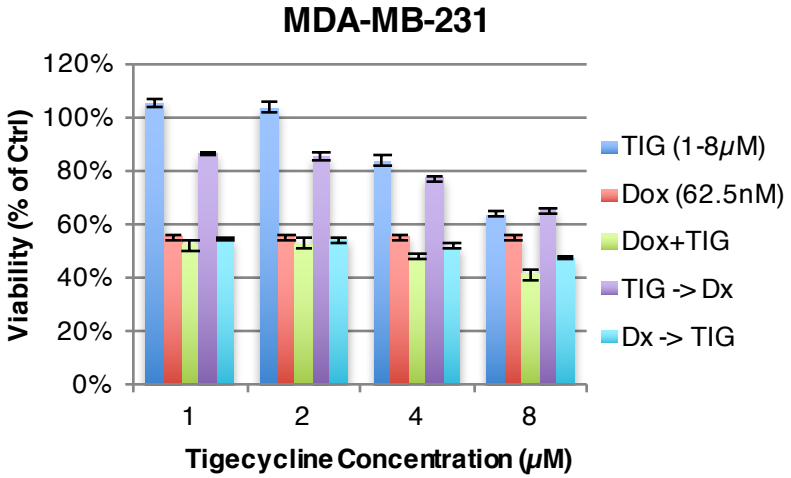

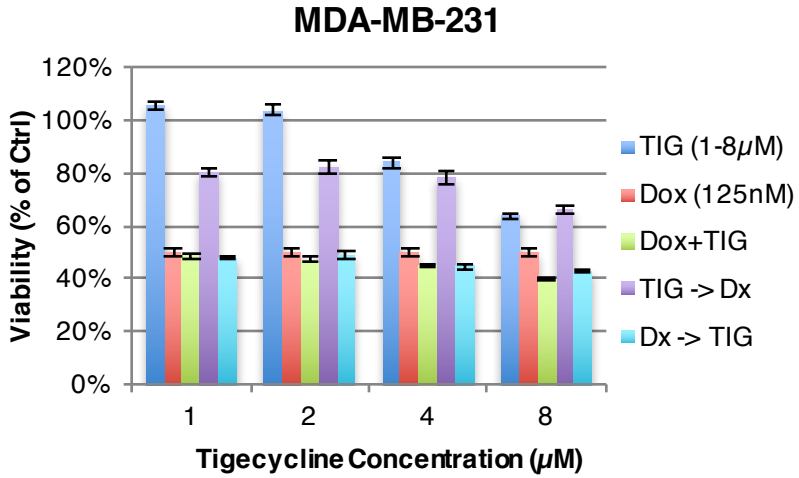

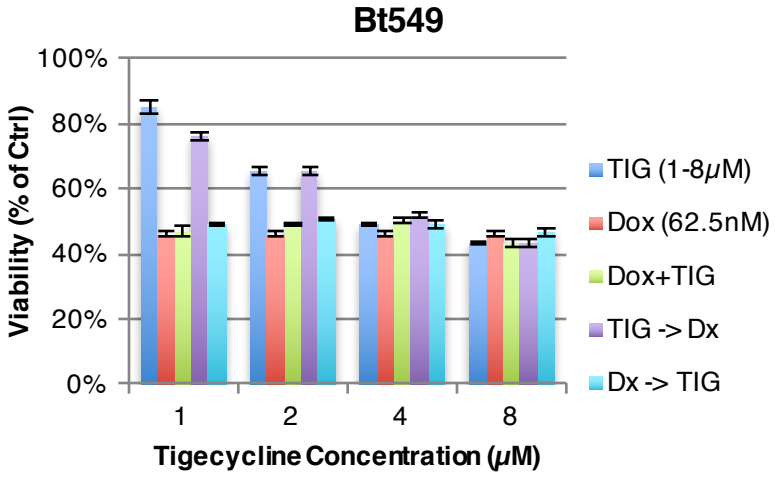

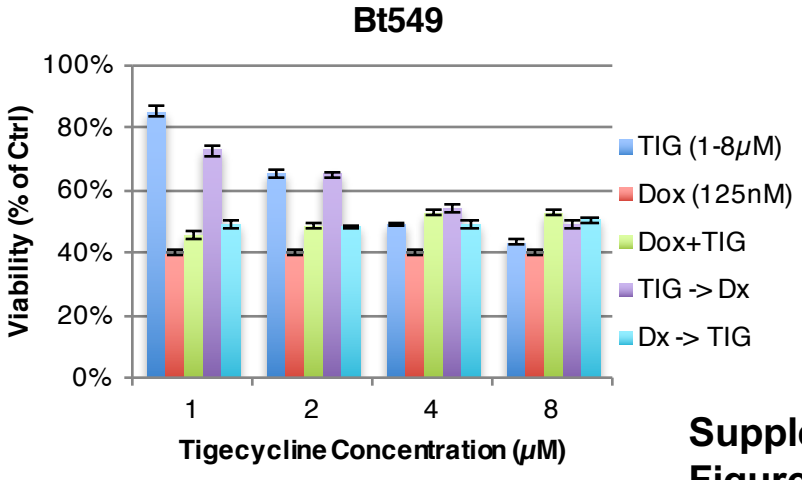

Supplemental Figure S10A-B

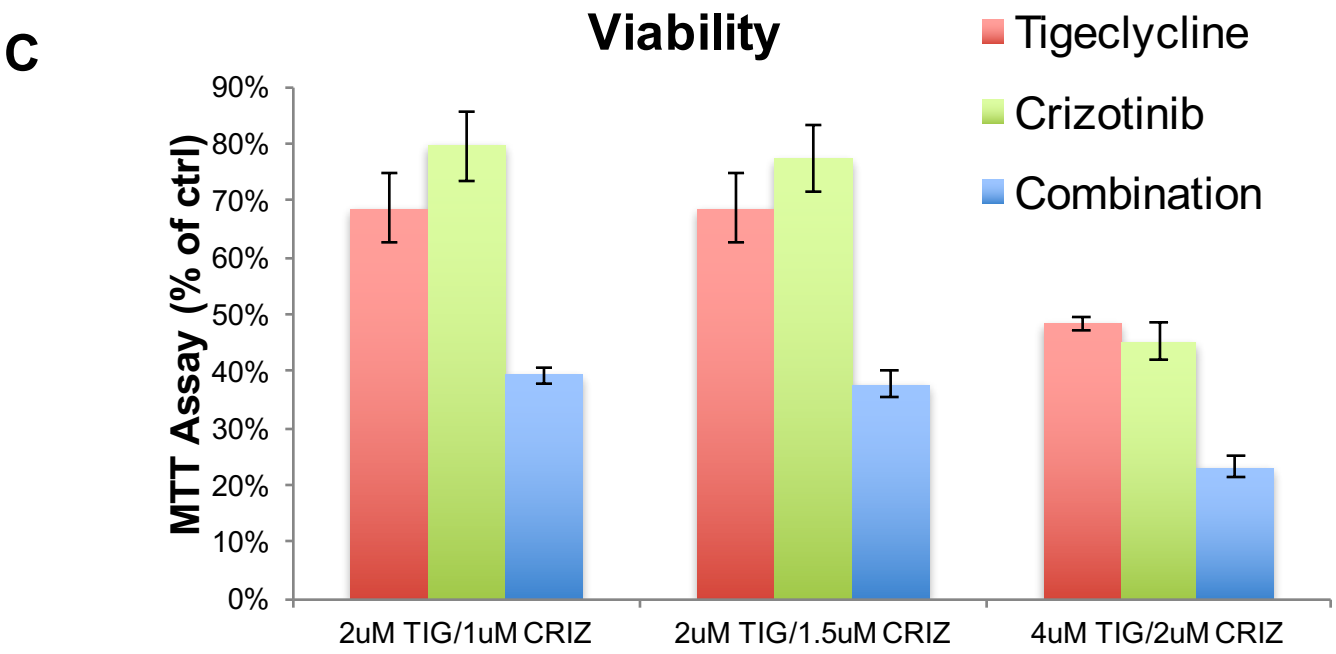

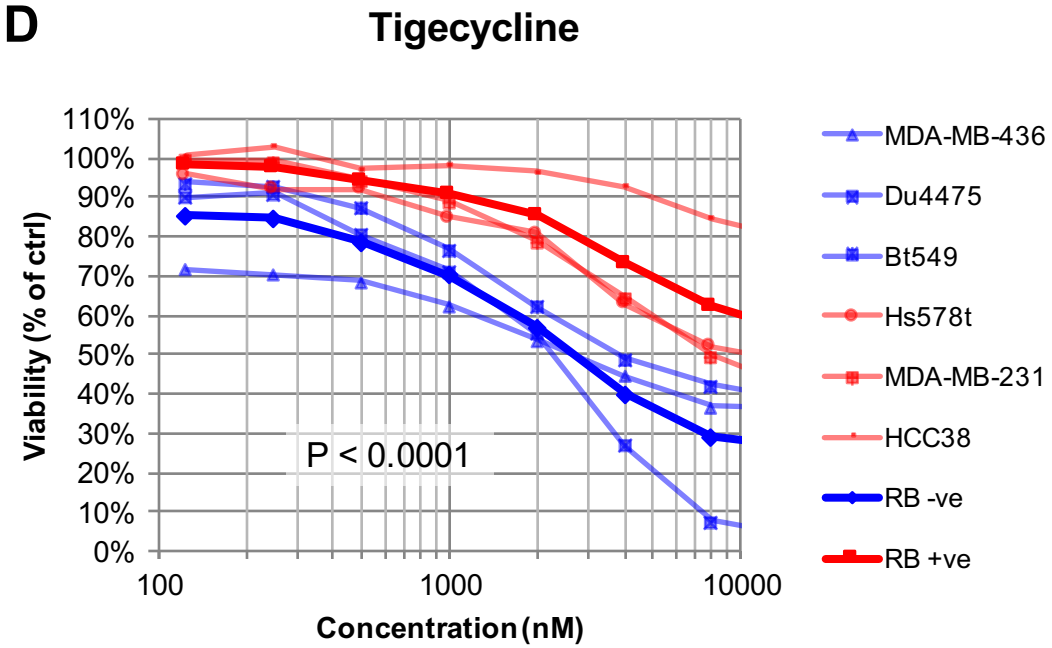

RB - vs RB +, p<0.0001

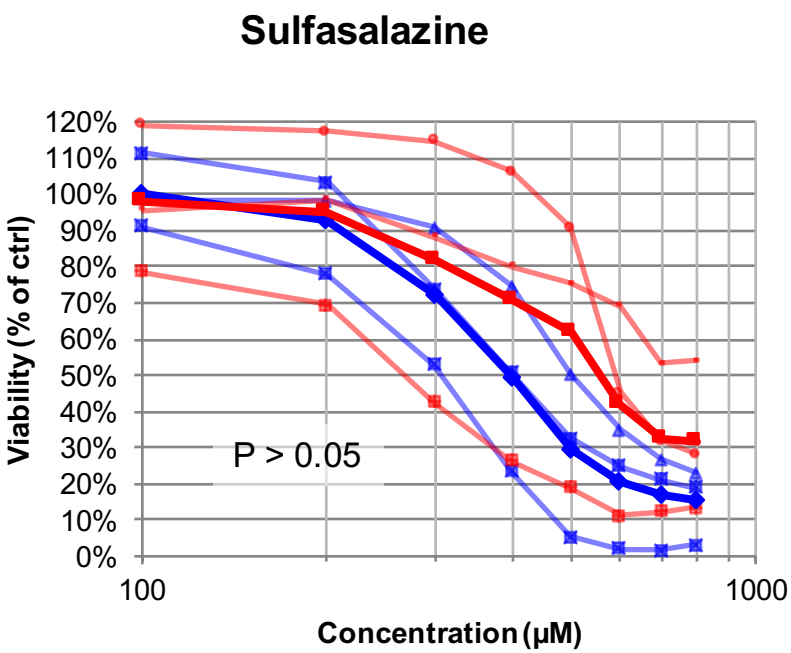

RB - vs RB +, p=0.1888

Supplemental Figure S10C-E

Figure S10. Effect of order-of-addition of TIG plus doxorubicin or SSZ on growth of TNBC cells. (**A**) MDA-MB-231 and Bt549 cells treated with tigecycline and doxorubicin alone or in combination were analyzed by MTT assays showing minimal cooperation between tigecycline and doxorubicin. (**B**) Effect of order-of-addition of tigecycline and/or doxorubicin on indicated TNBC lines. (**C**) Cooperative effect of TIG and the MET inhibitor crizotinib in BT549 TNBC cells. (**D-E**) TIG vs. SSZ treatment of indicated TNBC lines. Note that as opposed to TIG (Fig. 8D shown here for comparison), SSZ has insignificantly differential effects on growth of $RB^{+}/p53^{-}$ vs $RB^{-}/p53^{-}$ TNBC.

A

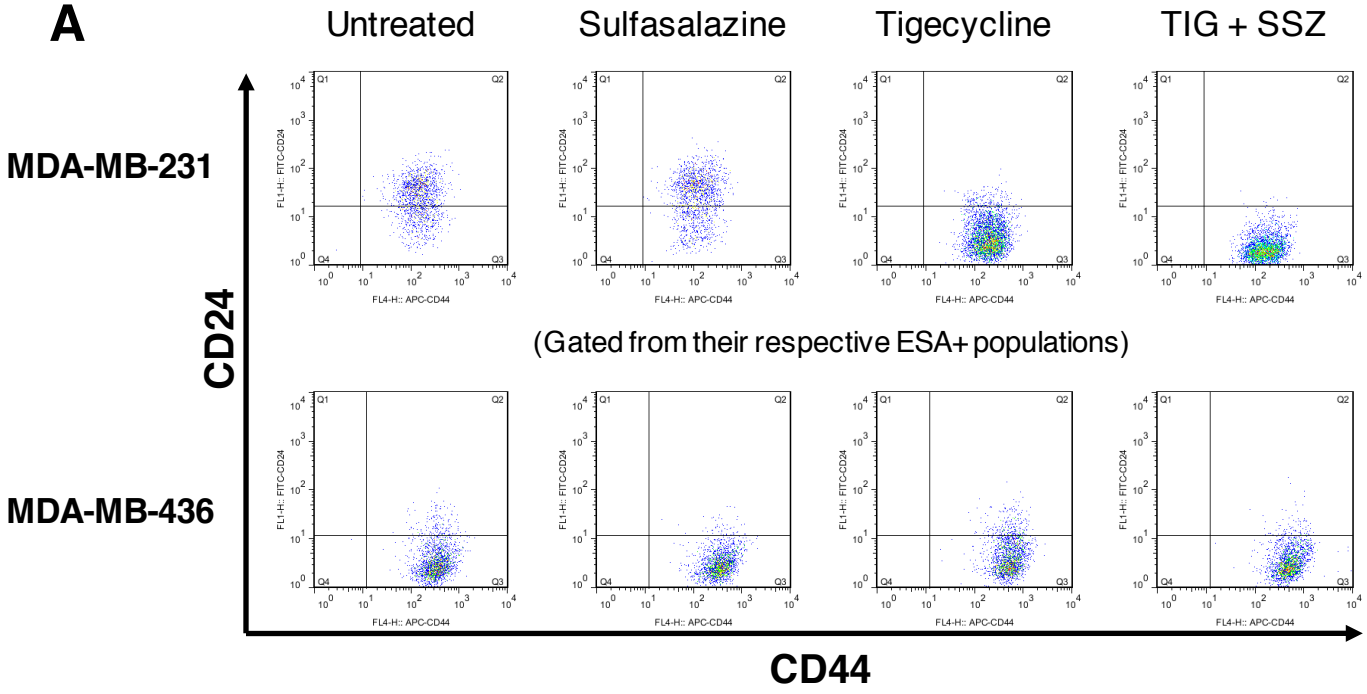

B

CSC Relative Ratio

	Untreated	SSZ	TIG	T+S
MDA-MB-231(RB+)	1.00	0.88	2.88	2.82
MDA-MB-436 (RB-)	1.00	1.14	1.05	1.09
HCC38 (RB+)	1.00	n/a	1.82	n/a
HCC1937 (RB-)	1.00	n/a	0.69	n/a

Supplemental Figure S11

Figure S11. TIG treatment increases the CSC fraction in RB^+ but not RB^- TNBC cells. (**A**) Representative flow cytometry analysis for the $CD24^-$:$CD44^+$:ESA^+ CSC fraction in the $RB^+/p53^-$ MDA-MB-231 vs. $RB^-/p53^-$ MDA-MB-436 TNBC lines after TIG +/- SSZ treatments. Shown are the CD24 and CD44 profile after gating on the ESA^+ cells. Note the increase in the CSC population after TIG treatment in RB^+ MDA-MB-231 cells. (**B**) Summary of the effects of TIG on the CSC fraction in two $RB^+/p53^-$ vs $RB^-/p53^-$ TNBC lines using IC_{50} drug concentrations.

MDA-MB-436

Xenografts in NSG (36 days treatment)

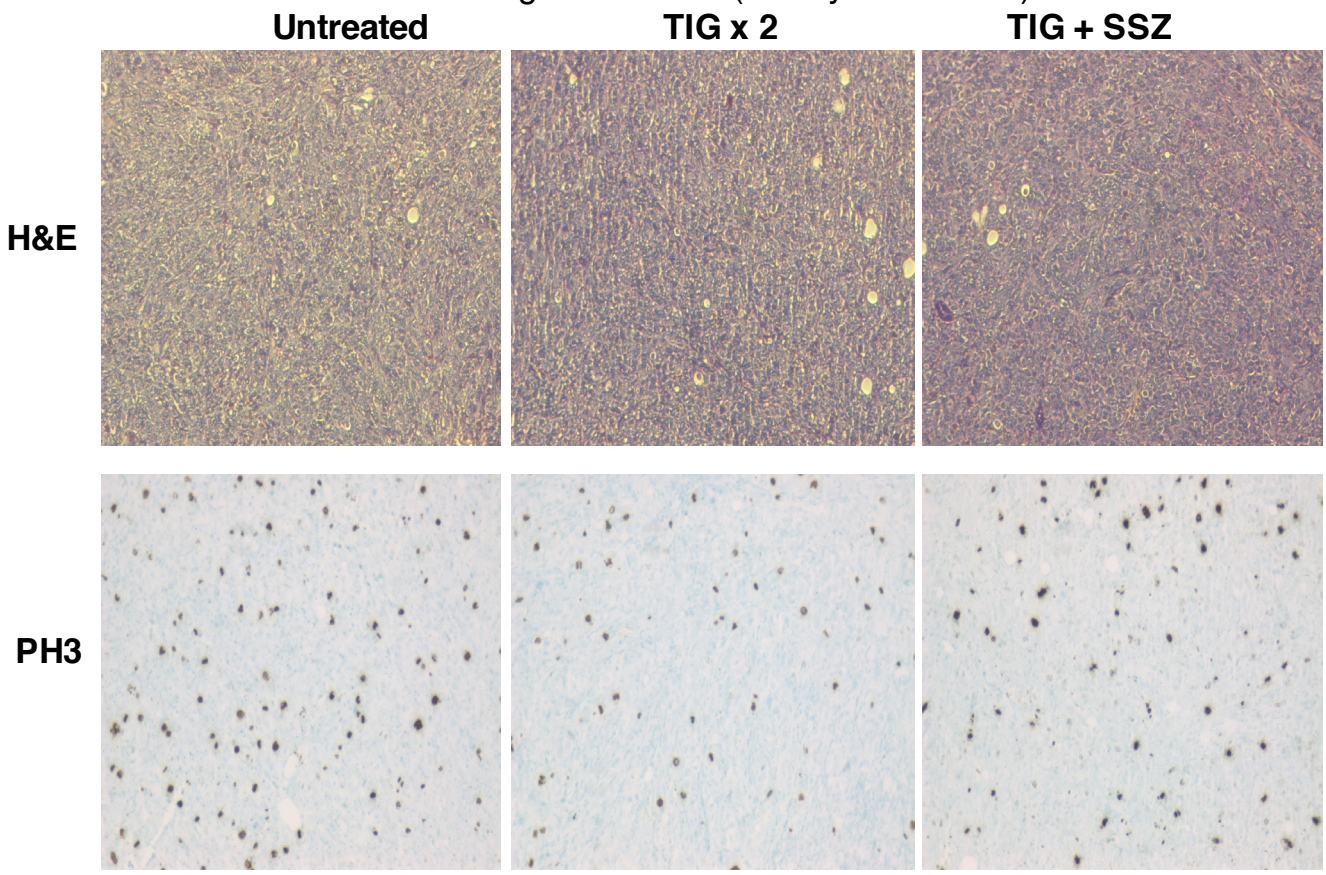

Supplemental Figure S12

Figure S12. Representative histology (A) and staining for the mitotic marker phospho-H3 (B) of sections from MDA-MB-436 xenografts treated or not with double dose of TIG or TIG + SSZ for 36 days. At day 36, T+S Ctrl n=4, T+S treatment n=4, TIGx2 ctrl n=4, TIGx2 treatment n=5. For each tumor 6 slides were analyzed. Note the reduced PH3 positive cells following TIG treatment. See quantification in Fig. 10F-G.

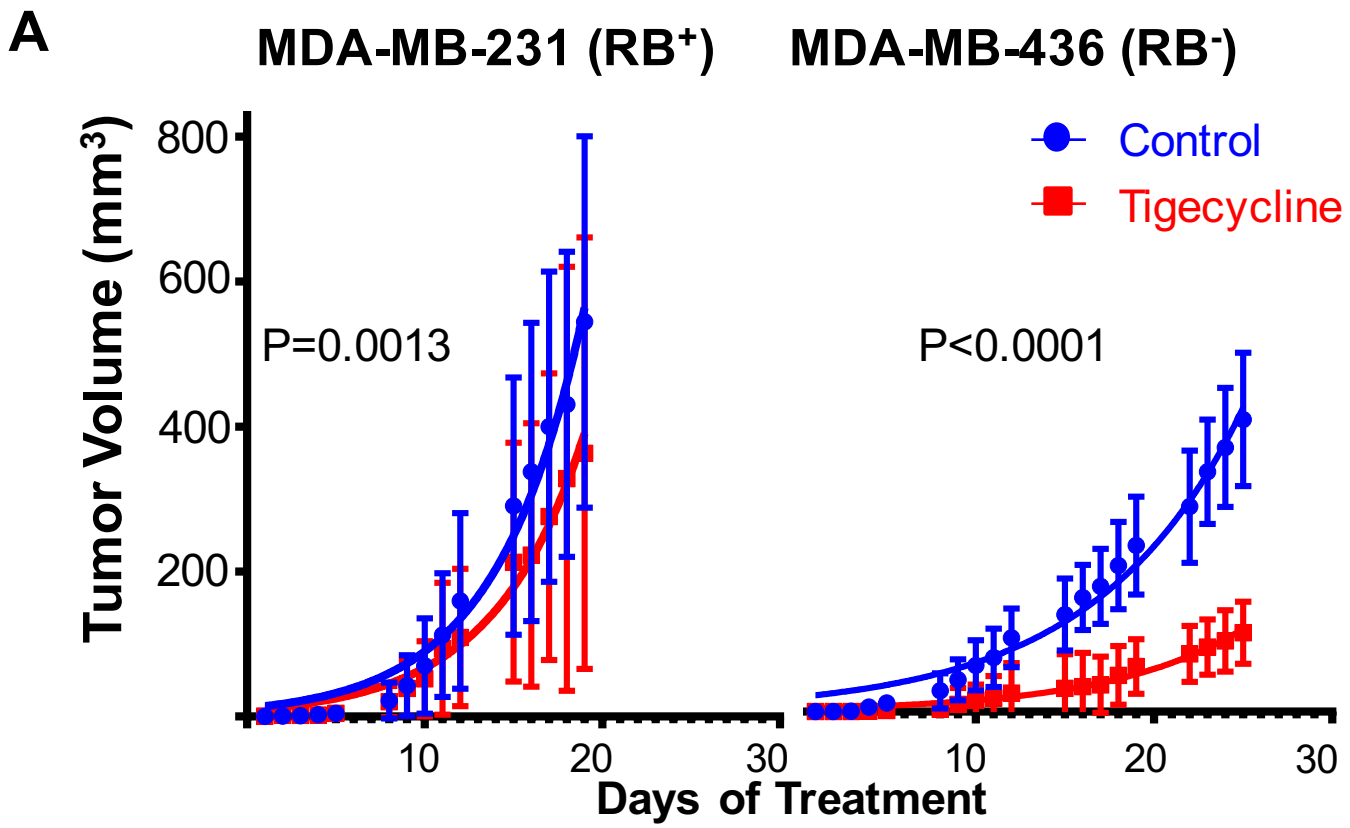

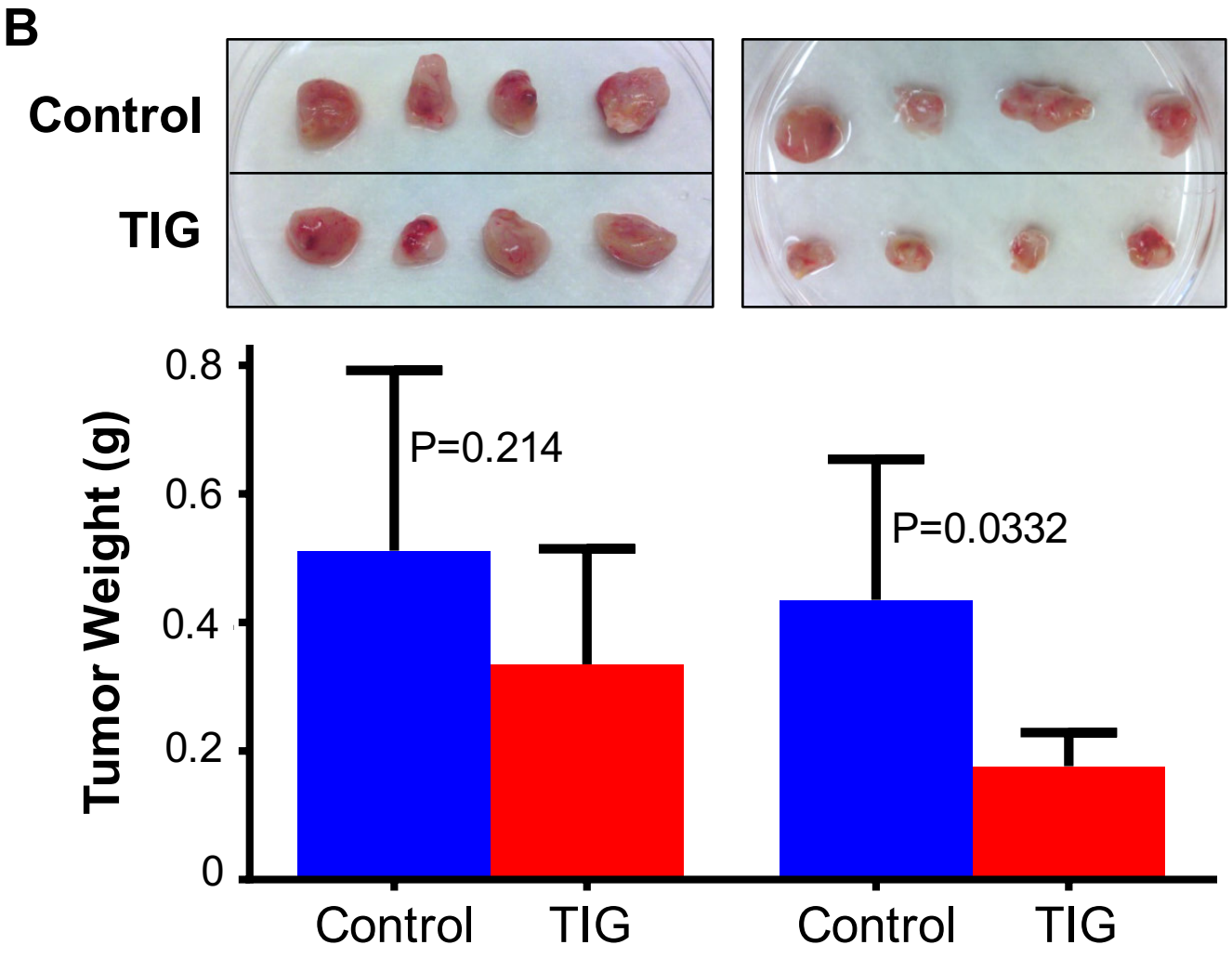

Supplemental Fig. S13

Figure S13. Efficient suppression of $RB^-/p53^-$ but not $RB^+/p53^-$ TNBC xenograft growth by tigecycline. (A) NSG mice were injected with $1x10^6$ MDA-MB-436 ($RB^-/p53^-$) or MDA-MB-231 ($RB^+/p53^-$) cells into their inguinal (#4) mammary gland. Once palpable tumors formed mice were treated with tigecycline (50mg/kg) (n=8) or PBS (Control) (n=6) twice daily. Tumor diameter was measured 5 days/week. p-values were calculated using the Wilcoxon method. (**B**) Tumors were excised, photographed and weighed. P values by student t-test.

MPT genes		
hATP5D	forward	TGGTCGTGGTGCATGCAG
	reverse	CAACATGTCCAGCGTCACG
hTOMM40	forward	GAGTTTGAGGCCAGCACAAG
	reverse	ACCCACGATCCAGTTGCTAT
hCISD1	forward	TACTGCCGTTGTTGGAGGTC
	reverse	ATCAGAGGGCCCACATTGTC
hDHFR	forward	AGCAGAGAACTCAAGGAACCT
	reverse	GCCACCAACTATCCAGACCA
hMRLP37	forward	TGGACTGTAACGAGGGTGTC
	reverse	TGTCTCTGGCTTGAAACCAAC
hNDUFAB1	forward	CAGCCGGCCTTAGTGCTC
	reverse	GGTCCTGGATGCCCTCTAAC
hNSUN4	forward	CAGGGATGGAAATCAAGTTCGA
	reverse	ATGAAGGGAGTGGCGGTC
hPHB2	forward	CTATGACATTCGGGCCAGAC
	reverse	CATTGGGTCGAGACAACACTC
Known E2F1 regulated genes		
hPOLalpha1	forward	GAAGTTCAAGTCTAAGCCAGTGG
	reverse	AGGCTAGATGTGTTGGTCCC
hTK1	forward	ATGCCAAAGACACTCGCTAC
	reverse	TCGTCGATGCCTATGACAGC
hCCNE1	forward	CAAAATCGACAGGACGGCG
	reverse	CTTGCACGTTGAGTTTGGGT
hBBC3	Forward	GATGGCGGACGACCTCAAC
	Reverse	TGATGAGATTGTACAGGACCCTC
others		
hGAPDH	forward	TGGAAGGACTCATGACCACAG
	reverse	ATGATGTTCTGGAGAGCCCC

Supplemental Figure S14

Figure S14. Q-rt-PCR primers used in this study for MPT, cell cycle, apoptosis and other genes.